


$P_{\psi s}^\Lambda(4459)$ and $P_{\psi s}^\Lambda(4338)$ as molecular states in $J/\psi\Lambda$ invariant mass spectraJun-Tao Zhu, Shu-Yi Kong, and Jun He^{*}*School of Physics and Technology, Nanjing Normal University, Nanjing 210097, China* (Received 14 November 2022; accepted 15 February 2023; published 27 February 2023)

Recently, the LHCb Collaboration has reported two strange hidden-charm pentaquark states named $P_{\psi s}^\Lambda(4459)$ and $P_{\psi s}^\Lambda(4338)$ in the $J/\psi\Lambda$ invariant mass spectra of decays $\Xi_b^- \rightarrow J/\psi\Lambda K^-$ and $B^- \rightarrow J/\psi\Lambda\bar{p}$, respectively. In this work, we perform a coupled-channel study of the interactions $\Xi_c^* \bar{D}^*$, $\Xi_c' \bar{D}^*$, $\Xi_c \bar{D}$, $\Xi_c \bar{D}^*$, $\Xi_c' \bar{D}$, $\Lambda_c \bar{D}_s^*$, $\Xi_c \bar{D}$, $\Lambda_c \bar{D}_s$, and $\Lambda J/\psi$ in the quasipotential Bethe-Salpeter equation approach to estimate the $J/\psi\Lambda$ invariant mass spectra. With the help of effective Lagrangians, the potential kernel can be constructed by meson exchanges to obtain the scattering amplitudes, from which the poles of the bound states and the invariant mass spectra can be reached. The coupled-channel calculation results in that the width of state $\Xi_c \bar{D}^*(1/2^-)$ is about 18 MeV and that of state $\Xi_c \bar{D}^*(3/2^-)$ is only about 1.6 MeV. By comparison with experimental data, it indicates that the structure $P_{\psi s}^\Lambda(4459)$ is mainly from the contribution from the $\Xi_c \bar{D}^*(1/2^-)$ state while the role of state $\Xi_c \bar{D}^*(3/2^-)$ cannot be excluded. The line shape of the structure $P_{\psi s}^\Lambda(4338)$ can be reproduced roughly by a narrow molecular state from the $\Xi_c \bar{D}$ interaction with $J^P = 1/2^-$, which is extremely close to the threshold, with a large interference effect. Besides, an additional state $\Xi_c' \bar{D}(1/2^-)$ is suggested to be observed as a dip structure in the $J/\psi\Lambda$ invariant mass spectrum.

DOI: [10.1103/PhysRevD.107.034029](https://doi.org/10.1103/PhysRevD.107.034029)**I. INTRODUCTION**

In the recent years, one of the most important experimental progresses of the exotic hadron studies is the observation of $P_{\psi}^N(4450)$ and $P_{\psi}^N(4380)$ at LHCb in 2015 [1], which were predicted by several theoretical groups [2–5]. Inspired by the experimental observation, more theoretical studies of the hidden-charm pentaquark structures emerge [6,7]. Subsequently, the $P_{\psi}^N(4450)$ was separated into two structures $P_{\psi}^N(4440)$ and $P_{\psi}^N(4457)$, and a new structure $P_{\psi}^N(4312)$ was observed at LHCb in 2019 [8]. The observations of three states with small widths and masses close to corresponding thresholds well illustrate the validity of the molecular state interpretation [9–14]. Furthermore, the theoretical studies about molecular states from nonstrange hidden-charm systems have been extent into hidden-charm pentaquark states with strangeness [15–23].

In 2020, the LHCb Collaboration reported a 3σ strange hidden-charm pentaquark structure $P_{\psi s}^\Lambda(4459)$ in the $\Xi_b^- \rightarrow J/\psi\Lambda K^-$ decay [24]. This structure has a mass of 19 MeV

below the $\Xi_c \bar{D}^*$ threshold and a width of 17 MeV [24], which is consistent with the properties of a molecular state. There are a wide variety of studies of the molecular state interpretation of $P_{\psi s}^\Lambda(4459)$ in the literature. In Ref. [25], the authors considered the molecular state interpretation for this state and concluded that it is either a $\Xi_c' \bar{D}$ state with $I(J^P) = 0(3/2^-)$, or a $\Xi_c \bar{D}^*$ state with $0(3/2^-)$. In Ref. [26], a calculation was also performed with the QCD sum rule, and the result supports the interpretation of $P_{\psi s}^\Lambda(4459)$ as a $\Xi_c \bar{D}^*$ molecular state with either $J^P = 1/2^-$ or $3/2^-$. In Ref. [27], it was suggested that its two-body strong decay behavior supports an assignment of $P_{\psi s}^\Lambda(4459)$ as a $\Xi_c \bar{D}^*$ state with $I(J^P) = 0(3/2^-)$. In Ref. [28], the results under the heavy quark spin symmetry (HQSS) limits also prefer $\Xi_c \bar{D}^*(3/2^-)$ to $\Xi_c \bar{D}^*(1/2^-)$ as the candidate of $P_{\psi s}^\Lambda(4459)$.

Very recently, the LHCb Collaboration reported their results about the $B^- \rightarrow J/\psi\Lambda\bar{p}$ decay, which indicates a new neutral strange hidden-charm pentaquark state named $P_{\psi s}^\Lambda(4338)$. It carries a mass of $4338.3 \pm 0.7 \pm 0.4$ MeV and a width of $7.0 \pm 1.2 \pm 1.3$ MeV [29]. Since its mass and narrow width are in good line with the properties of molecular state, many new researches about the $P_{\psi s}^\Lambda(4338)$ also suggest it as a molecular state [30–37]. In Ref. [35], a pole corresponding to $P_{\psi s}^\Lambda(4338)$ and an additional pole $P_{\psi s}^\Lambda(4254)$ near the $\Lambda_c \bar{D}_s$ threshold were found important to reproduce the experimental data. However, in Ref. [38],

^{*}Corresponding author.
junhe@njnu.edu.cn

Published by the American Physical Society under the terms of the [Creative Commons Attribution 4.0 International license](https://creativecommons.org/licenses/by/4.0/). Further distribution of this work must maintain attribution to the author(s) and the published article's title, journal citation, and DOI. Funded by SCOAP³.

the sharp $P_{\psi_s}^\Lambda(4338)$ enhancement is due to the triangle singularity in another diagram featuring a $1/2^-$ baryon consistent with $\Sigma_c(2800)$. In Ref. [39], the author studied the double thresholds distort the line shapes of the $P_{\psi_s}^\Lambda(4338)$ resonance in depth, and pointed out that it is misleading to depict the line shapes with Breit-Wigner distribution.

Within a quasipotential Bethe-Salpeter equation (qBSE) approach, possible molecular states from the $\Xi_c^{(\prime,*)}\bar{D}^{(*)}$ interactions were studied in our previous work [40]. The mass of the molecular state $\Xi_c\bar{D}^*(3/2^-)$ is very close to the mass of $P_{\psi_s}^\Lambda(4459)$, but its widths is narrower than the experimental results. The results do not exclude the possibility of two-pole structure from $\Xi_c\bar{D}^*$ states with $1/2^-$ and $3/2^-$ and the role of either state in reproducing the experimental invariant mass spectrum. It is worth mentioning that our previous work also predicts other partners of $P_{\psi_s}^\Lambda(4459)$ from the $\Xi_c^{(\prime,*)}\bar{D}^{(*)}$ interaction, including a molecular state from the $\Xi_c\bar{D}$ interaction with $1/2^-$ [40], which has a mass close to the $P_{\psi_s}^\Lambda(4338)$ observed in the recent LHCb experiment [29].

In the previous work, only the $\Xi_c^{(\prime,*)}\bar{D}^{(*)}$ channels which can produce bound states were considered, and the coupling effects of unbound channels were not included, especially the $\Lambda J/\psi$ channel where the strange hidden-charm pentaquarks $P_{\psi_s}^\Lambda(4459)$ and $P_{\psi_s}^\Lambda(4338)$ were observed. In the current work, a coupled-channel calculation will be performed to estimate roles of the molecular states in the $J/\psi\Lambda$ invariant mass spectrum and their relations to the observed structures. To obtain more reasonable mass and width, the full coupled-channels effects for the $P_{\psi_s}^\Lambda$ states are completely considered, including channels $\Xi_c^{(\prime,*)}\bar{D}^{(*)}$, $\Lambda_c\bar{D}_s^{(*)}$, and $\Lambda J/\psi$. By comparison with experimental data, the origins of the $P_{\psi_s}^\Lambda(4459)$ and $P_{\psi_s}^\Lambda(4338)$ will be discussed.

After the introduction, Lagrangians used to construct the potential of couple-channel interaction, the qBSE approach, and formula of the invariant mass spectrum will be presented in Sec. II. In Sec. III, single-channel calculation results, coupled-channel calculation results, and the estimations of the $J/\psi\Lambda$ invariant mass spectrums will be given and discussed, respectively. Section IV is a summary of the whole work and some suggestions for experiment.

II. FORMALISM

We will search for the poles in the complex energy plane within qBSE approach, and compare the results with the

$J/\psi\Lambda$ invariant mass spectrum. Hence, the potential kernel should be constructed first with effective Lagrangians to calculate the scattering amplitudes, which are used to found the poles and estimate the invariant mass spectra.

A. Relevant Lagrangians and potentials

In the current work, we consider all hidden-charm channels relevant to the $P_{\psi_s}^\Lambda$, which explicitly include $\Xi_c^*\bar{D}^*$, $\Xi_c'\bar{D}^*$, $\Xi_c^*\bar{D}$, $\Xi_c\bar{D}^*$, $\Xi_c'\bar{D}$, $\Lambda_c\bar{D}_s^*$, $\Xi_c\bar{D}$, $\Lambda_c\bar{D}_s$, and $\Lambda J/\psi$. For the former eight channels, we need the Lagrangians under the heavy quark limit and chiral symmetry [40–44],

$$\begin{aligned}
\mathcal{L}_{\tilde{P}^*\tilde{P}\mathbb{P}} &= i\frac{2g\sqrt{m_{\tilde{P}}m_{\tilde{P}^*}}}{f_\pi}(-\tilde{P}_{a\lambda}^{*\dagger}\tilde{P}_b + \tilde{P}_a^\dagger\tilde{P}_{b\lambda}^*)\partial^\lambda\mathbb{P}_{ab}, \\
\mathcal{L}_{\tilde{P}^*\tilde{P}^*\mathbb{P}} &= -\frac{g}{f_\pi}\epsilon_{\alpha\mu\nu\lambda}\tilde{P}_a^{*\mu\dagger}\overset{\leftrightarrow}{\partial}^\alpha\tilde{P}_b^{*\lambda}\partial^\nu\mathbb{P}_{ba}, \\
\mathcal{L}_{\tilde{P}^*\tilde{P}\mathbb{V}} &= \sqrt{2}\lambda g_V\epsilon_{\lambda\alpha\beta\mu}(-\tilde{P}_a^{*\mu\dagger}\overset{\leftrightarrow}{\partial}^\lambda\tilde{P}_b + \tilde{P}_a^\dagger\overset{\leftrightarrow}{\partial}^\lambda\tilde{P}_b^{*\mu})(\partial^\alpha\mathbb{V}^\beta)_{ab}, \\
\mathcal{L}_{\tilde{P}\tilde{P}\mathbb{V}} &= i\frac{\beta g_V}{\sqrt{2}}\tilde{P}_a^\dagger\overset{\leftrightarrow}{\partial}_\mu\tilde{P}_b\mathbb{V}_{ab}^\mu, \\
\mathcal{L}_{\tilde{P}^*\tilde{P}^*\mathbb{V}} &= -i\frac{\beta g_V}{\sqrt{2}}\tilde{P}_a^{*\dagger}\overset{\leftrightarrow}{\partial}_\mu\tilde{P}_b^{*\mu}\mathbb{V}_{ab}^\mu \\
&\quad - i2\sqrt{2}\lambda g_V m_{\tilde{P}^*}\tilde{P}_a^{*\mu\dagger}\tilde{P}_b^{*\nu}(\partial_\mu\mathbb{V}_\nu - \partial_\nu\mathbb{V}_\mu)_{ab}, \\
\mathcal{L}_{\tilde{P}\tilde{P}\sigma} &= -2g_s m_{\tilde{P}}\tilde{P}_a^\dagger\tilde{P}_a\sigma, \\
\mathcal{L}_{\tilde{P}^*\tilde{P}^*\sigma} &= 2g_s m_{\tilde{P}^*}\tilde{P}_a^{*\dagger}\tilde{P}_a^*\sigma,
\end{aligned} \tag{1}$$

where the $\tilde{P} = (\bar{D}^0, D^-, D_s^-)$, and the \mathbb{P} and \mathbb{V} are the pseudoscalar and vector matrices as

$$\begin{aligned}
\mathbb{P} &= \begin{pmatrix} \frac{\sqrt{3}\pi^0 + \eta}{\sqrt{6}} & \pi^+ & K^+ \\ \pi^- & \frac{-\sqrt{3}\pi^0 + \eta}{\sqrt{6}} & K^0 \\ K^- & \bar{K}^0 & -\frac{2\eta}{\sqrt{6}} \end{pmatrix}, \\
\mathbb{V} &= \begin{pmatrix} \frac{\rho^0 + \omega}{\sqrt{2}} & \rho^+ & K^{*+} \\ \rho^- & \frac{-\rho^0 + \omega}{\sqrt{2}} & K^{*0} \\ K^{*-} & \bar{K}^{*0} & \phi \end{pmatrix}.
\end{aligned} \tag{2}$$

where the indices $a, b = 1, 2, 3$ are used to label the particle elements in the matrices \mathbb{P} , \mathbb{V} , and vector \mathcal{P} .

Then, the Lagrangians for the couplings between charmed baryon and light mesons can also be given as,

$$\begin{aligned}
 \mathcal{L}_{BBP} &= -i \frac{3g_1}{4f_\pi \sqrt{m_B m_B}} \epsilon^{\mu\nu\lambda\kappa} \partial_\nu \mathbb{P} \sum_{i,j=0,1} \bar{B}_i^\mu \overleftrightarrow{\partial}_\kappa B_{j\lambda}, \\
 \mathcal{L}_{BBV} &= -\frac{\beta_S g_V}{2\sqrt{2} m_B m_B} \mathbb{V}^\nu \sum_{i,j=0,1} \bar{B}_i^\mu \overleftrightarrow{\partial}_\nu B_{j\mu} \\
 &\quad - \frac{\lambda_S g_V}{\sqrt{2}} (\partial_\mu \mathbb{V}_\nu - \partial_\nu \mathbb{V}_\mu) \sum_{i,j=0,1} \bar{B}_i^\mu B_j^\nu, \\
 \mathcal{L}_{BB\sigma} &= \ell_S \sigma \sum_{i,j=0,1} \bar{B}_i^\mu B_{j\mu}, \\
 \mathcal{L}_{B_3 B_3 \mathbb{V}} &= -\frac{g_V \beta_B}{2\sqrt{2} m_{B_3} m_{B_3}} \mathbb{V}^\mu \bar{B}_3^\mu \overleftrightarrow{\partial}_\mu B_3, \\
 \mathcal{L}_{B_3 B_3 \sigma} &= i \ell_B \sigma \bar{B}_3 B_3, \\
 \mathcal{L}_{BB_3 \mathbb{P}} &= -i \frac{g_4}{f_\pi} \sum_i \bar{B}_i^\mu \partial_\mu \mathbb{P} B_3 + \text{H.c.}, \\
 \mathcal{L}_{BB_3 \mathbb{V}} &= \frac{g_V \lambda_1}{\sqrt{2} m_B m_{B_3}} \epsilon^{\mu\nu\lambda\kappa} \partial_\lambda \mathbb{V}_\kappa \sum_i \bar{B}_i^\mu \overleftrightarrow{\partial}_\nu B_3 + \text{H.c.}, \quad (3)
 \end{aligned}$$

where the Dirac spinor operators with label $i, j = 0, 1$ are defined as,

$$\begin{aligned}
 B_{0\mu} &\equiv -\sqrt{\frac{1}{3}} (\gamma_\mu + v_\mu) \gamma^5 B; & B_{1\mu} &\equiv B_\mu^{*ab}, \\
 \bar{B}_{0\mu} &\equiv \sqrt{\frac{1}{3}} \bar{B} \gamma^5 (\gamma_\mu + v_\mu); & \bar{B}_{1\mu} &\equiv \bar{B}_\mu^*. \quad (4)
 \end{aligned}$$

and the charmed baryon matrices are defined as

$$\begin{aligned}
 B_3 &= \begin{pmatrix} 0 & \Lambda_c^+ & \Xi_c^+ \\ -\Lambda_c^+ & 0 & \Xi_c^0 \\ -\Xi_c^+ & -\Xi_c^0 & 0 \end{pmatrix}, \\
 B &= \begin{pmatrix} \Sigma_c^{++} & \frac{1}{\sqrt{2}} \Sigma_c^+ & \frac{1}{\sqrt{2}} \Xi_c^+ \\ \frac{1}{\sqrt{2}} \Sigma_c^+ & \Sigma_c^0 & \frac{1}{\sqrt{2}} \Xi_c^0 \\ \frac{1}{\sqrt{2}} \Xi_c^+ & \frac{1}{\sqrt{2}} \Xi_c^0 & \Omega_c^0 \end{pmatrix}, \\
 B^* &= \begin{pmatrix} \Sigma_c^{*++} & \frac{1}{\sqrt{2}} \Sigma_c^{*+} & \frac{1}{\sqrt{2}} \Xi_c^{*+} \\ \frac{1}{\sqrt{2}} \Sigma_c^{*+} & \Sigma_c^{*0} & \frac{1}{\sqrt{2}} \Xi_c^{*0} \\ \frac{1}{\sqrt{2}} \Xi_c^{*+} & \frac{1}{\sqrt{2}} \Xi_c^{*0} & \Omega_c^{*0} \end{pmatrix}. \quad (5)
 \end{aligned}$$

The masses of particles involved in the calculation are chosen as suggested central values in the Review of Particle Physics (PDG) [45]. The mass of broad σ meson is chosen as 500 MeV. The coupling constants involved are listed in Table I.

However, for the couplings of former eight channels and the lowest channel $\Lambda J/\psi$, the heavy quark effective Lagrangians are not enough for calculation. Here, we apply effective Lagrangians under the SU(4) symmetry as [50–53],

TABLE I. The coupling constants adopted in the calculation, which are cited from the literature [46–49]. The λ and $\lambda_{S,I}$ are in the units of GeV^{-1} . Others are in the units of 1.

β	g	g_V	λ	g_s	ℓ_S	
0.9	0.59	5.9	0.56	0.76	6.2	
β_S	g_1	λ_S	β_B	ℓ_B	g_4	λ_I
-1.74	-0.94	-3.31	$-\beta_S/2$	$-\ell_S/2$	$3g_1/(2\sqrt{2})$	$-\lambda_S/\sqrt{8}$

$$\begin{aligned}
 \mathcal{L}_{BBP} &= \frac{g_{BBP}}{m_P} \bar{B} \gamma^\mu \gamma^5 \partial_\mu P B, \\
 \mathcal{L}_{BBV} &= -g_{BBV} \bar{B} \gamma^\mu V_\mu B, \\
 \mathcal{L}_{BB^*P} &= \frac{g_{BB^*P}}{m_P} (\bar{B}^{*\mu} B + \bar{B} B^{*\mu}) \partial_\mu P, \\
 \mathcal{L}_{BB^*V} &= -i \frac{g_{BB^*V}}{m_V} (\bar{B}^{*\mu} \gamma^5 \gamma^\nu B - \bar{B} \gamma^5 \gamma^\nu B^{*\mu}) \\
 &\quad \times (\partial_\mu V_\nu - \partial_\nu V_\mu), \\
 \mathcal{L}_{PPV} &= -g_{PPV} (P \partial_\mu P - \partial_\mu P P) V^\mu, \\
 \mathcal{L}_{VVP} &= \frac{g_{VVP}}{m_V} \epsilon_{\mu\nu\alpha\beta} \partial^\mu V^\nu \partial^\alpha V^\beta P, \\
 \mathcal{L}_{VVV} &= g_{VVV} \langle (\partial_\mu V_\nu - \partial_\nu V_\mu) V^\mu V^\nu \rangle, \quad (6)
 \end{aligned}$$

where the involved coupling constants are shown in Table II.

With the vertices obtained from above Lagrangians, the potential of couple-channel interaction can be constructed easily with the help of the standard Feynman rules. Because nine channels are involved in the current work, it is tedious

TABLE II. The coupling constants determined with SU(4) symmetry, and $g_{B^*BV} = 16.03$, $g_{B^*BP} = 2.127$, $g_{BBV} = 3.25$, $g_{BBP} = 0.989$, $g_{PPV} = 3.02$, $g_{VVP} = -7.07$, and $g_{VVV} = 2.298$ [53]. The values are in the units of GeV.

Coupling constant	Relation	Values
$g_{\Xi_c^* \Lambda D^*}$	$\frac{1}{2} g_{B^*BV}$	8.015
$g_{\Xi_c^* \Lambda D^*}$	$-\sqrt{\frac{3}{2}} g_{BBV}$	-3.98
$g_{\Xi_c^* \Lambda D^*}$	$-\frac{1}{\sqrt{2}} g_{BBV}$	-2.298
$g_{\Lambda_c \Lambda D_s^*}$	$\sqrt{2} g_{BBV}$	4.596
$g_{D^* J/\psi D^*}$	g_{VVV}	2.298
$g_{D^* DJ/\psi}$	g_{VVP}	-7.07
$g_{DDJ/\psi}$	$-\sqrt{2} g_{PPV}$	-4.27
$g_{\Xi_c^* \Lambda D}$	$\frac{1}{2} g_{B^*BP}$	1.109
$g_{\Xi_c^* \Lambda D}$	$\frac{\sqrt{3}}{5\sqrt{2}} g_{BBP}$	0.242
$g_{\Xi_c^* \Lambda D}$	$-\frac{\sqrt{3}}{5\sqrt{2}} g_{BBP}$	-0.242
$g_{\Lambda_c \Lambda D_s}$	$\frac{3\sqrt{2}}{5} g_{BBP}$	0.839
$g_{D_s^* J/\psi D_s^*}$	g_{VVV}	2.298
$g_{D_s^* D_s J/\psi}$	g_{VVP}	-7.07
$g_{D_s D_s J/\psi}$	$-\sqrt{2} g_{PPV}$	-4.27

TABLE III. The flavor factors f_I for certain meson exchanges of certain interaction with isospin $I = 0$. The vertex for three pseudoscalar mesons should be forbidden.

	π	η	ρ	ω	σ
$\bar{D}^{(*)}\Xi_c^{(\prime,*)} \rightarrow \bar{D}^{(*)}\Xi_c^{(\prime,*)}$	-3/4	-1/12	-3/4	1/4	1
$\bar{D}^{(*)}\Xi_c \rightarrow \bar{D}^{(*)}\Xi_c$			-3/2	1/2	2
$\bar{D}^{(*)}\Xi_c \rightarrow \bar{D}^{(*)}\Xi_c^{(\prime,*)}$	$-3\sqrt{2}/4$	$-\sqrt{2}/4$	$-3\sqrt{2}/4$	$\sqrt{2}/4$	
	K	K^*			
$\bar{D}^{(*)}\Xi_c^{(\prime,*)} \rightarrow \bar{D}_s^{(*)}\Lambda_c$	-1	-1			
$\bar{D}^{(*)}\Xi_c \rightarrow \bar{D}_s^{(*)}\Lambda_c$		$\sqrt{2}$			
	D	D^*	D_s	D_s^*	
$\bar{D}^{(*)}\Xi_c \rightarrow J/\psi\Lambda$	$-\sqrt{2}$	$-\sqrt{2}$			
$\bar{D}^{(*)}\Xi_c^{(\prime,*)} \rightarrow J/\psi\Lambda$	$-\sqrt{2}$	$-\sqrt{2}$			
$\bar{D}_s^{(*)}\Lambda_c \rightarrow J/\psi\Lambda$			1	1	

and fallible to give explicit 81 potential elements and input them into code. Instead, in this work, following the method in Refs. [54], we input vertices Γ and propagators P into the code directly. The potential can be written as

$$\mathcal{V}_{P,\sigma} = f_I \Gamma_1 \Gamma_2 P_{P,\sigma} f(q^2), \quad \mathcal{V}_V = f_I \Gamma_{1\mu} \Gamma_{2\nu} P_V^{\mu\nu} f(q^2). \quad (7)$$

The propagators are defined as usual as

$$P_{P,\sigma} = \frac{i}{q^2 - m_{P,\sigma}^2}, \quad P_V^{\mu\nu} = i \frac{-g^{\mu\nu} + q^\mu q^\nu / m_V^2}{q^2 - m_V^2}, \quad (8)$$

where the form factor $f(q^2)$ is adopted to compensate the off-shell effect of exchanged meson as $f(q^2) = e^{-(m_e^2 - q^2)/\Lambda_e^2}$ with m_e and q being the mass and momentum of the exchanged meson, respectively. And Λ_e is a cutoff to suppress the on-shell effect of exchange meson. In the propagator of exchanged meson, we make a replacement $q^2 \rightarrow -|q|^2$ to remove singularities as in Ref. [55]. The f_I is the flavor factor for certain meson exchange of certain interaction with isospin $I = 0$, and the explicit values are listed in Table III.

B. The qBSE approach

The Bethe-Salpeter equation is a four-dimensional integral equation in the Minkowski space, which is hard to solve directly. By using spectator quasipotential approximation and partial-wave decomposition, the four-dimensional equation can be reduced into a 1-dimensional equation with fixed spin-parity J^P as [56–58],

$$i\mathcal{M}_{\lambda'\lambda}^{J^P}(\mathbf{p}', \mathbf{p}) = i\mathcal{V}_{\lambda'\lambda}^{J^P}(\mathbf{p}', \mathbf{p}) + \sum_{\lambda''} \int \frac{\mathbf{p}''^2 d\mathbf{p}''}{(2\pi)^3} \cdot i\mathcal{V}_{\lambda'\lambda''}^{J^P}(\mathbf{p}', \mathbf{p}'') G_0(\mathbf{p}'') i\mathcal{M}_{\lambda''\lambda}^{J^P}(\mathbf{p}'', \mathbf{p}), \quad (9)$$

where the sum extends only over nonnegative helicity λ'' . The $G_0(\mathbf{p}'')$ is reduced from the 4-dimensional propagator under quasipotential approximation as $G_0(\mathbf{p}'') = \delta^+(p''_h^2 - m_h^2)/(p''_l^2 - m_l^2)$ with $p''_{h,l}$ and $m_{h,l}$ being the momenta and masses of heavy or light constituent particles. The partial wave potential is defined as,

$$\mathcal{V}_{\lambda'\lambda}^{J^P}(\mathbf{p}', \mathbf{p}) = 2\pi \int d\cos\theta [d_{\lambda'\lambda}^J(\theta) \mathcal{V}_{\lambda'\lambda}(\mathbf{p}', \mathbf{p}) + \eta d_{-\lambda'\lambda}^J(\theta) \mathcal{V}_{\lambda'-\lambda}(\mathbf{p}', \mathbf{p})], \quad (10)$$

where $\eta = PP_1P_2(-1)^{J-J_1-J_2}$ with P and J being parity and spin for system, constitution 1 or 2. The initial and final relative momenta are chosen as $\mathbf{p} = (0, 0, p)$ and $\mathbf{p}' = (p' \sin\theta, 0, p' \cos\theta)$. The $d_{\lambda'\lambda}^J(\theta)$ is the Wigner d-matrix and the integration of the amplitude is

$$\sum_{\lambda'\lambda} \int d\Omega |\mathcal{M}_{\lambda'\lambda}(\mathbf{p}', \mathbf{p})|^2 = \sum_{J^P, \lambda' \geq 0, \lambda \geq 0} |\hat{\mathcal{M}}_{\lambda'\lambda}^{J^P}(\mathbf{p}', \mathbf{p})|^2. \quad (11)$$

To solve the integral equation (9), we discretize the momenta \mathbf{p} , \mathbf{p}' , and \mathbf{p}'' by the Gauss quadrature with a weight $w(p_i)$ and have the discretized qBSE of the form as [56]

$$M_{ik} = V_{ik} + \sum_{j=0}^N V_{ij} G_j M_{jk}. \quad (12)$$

The propagator G is of a form

$$G_{j>0} = \frac{w(\mathbf{p}_j) \mathbf{p}_j''^2}{(2\pi)^3} G_0(\mathbf{p}_j''),$$

$$G_{j=0} = -\frac{i\mathbf{p}_o''}{32\pi^2 W} + \sum_j \left[\frac{w(\mathbf{p}_j)}{(2\pi)^3} \frac{\mathbf{p}_o''^2}{2W(\mathbf{p}_j''^2 - \mathbf{p}_o''^2)} \right], \quad (13)$$

where on-shell momentum $\mathbf{p}_o'' = \lambda^{1/2}(W, M_1, M_2)/2W$ with $\lambda(x, y, z) = [x^2 - (y+z)^2][x^2 - (y-z)^2]$ and W being the total energy of the system of two constituents. We also adopt an exponential regularization by introducing a form factor into the propagator as $G_0(\mathbf{p}'') \rightarrow G_0(\mathbf{p}'') [e^{-(p''_l^2 - m_l^2)/\Lambda_r^4}]^2$ with Λ_r being a cutoff [56]. For simply, we set the cutoff $\Lambda_e = \Lambda_r = \Lambda$ and adjust the value of Λ around 1 GeV. However, the key observation channel $\Lambda J/\psi$ couples with other channels only depend on the charmed heavy mesons like D, D_s, D^*, D_s^* . The cutoff $\Lambda_{(D, D_s)}$ and $\Lambda_{(D^*, D_s^*)}$ will be chosen at least larger than their masses. Specific values will be mentioned later.

The poles of nine-channel scattering amplitudes with different spin parities J^P are searched by variation of z in the complex energy plane to satisfy $|1 - V(z)G(z)| = 0$. For N channels calculation, there are a total number of 2^N Riemann sheets related to unitarity. In the current work, the

treatment in Ref. [59] is adopted to search for the poles. In such treatment, the default propagator $G(z)$ is adopted in energy region below the threshold and the $G(z) + ip_o''/16\pi^2 z$ for region above threshold, which correspond to the first and second Riemann sheets, respectively.

The amplitudes of $\Lambda J/\psi$ scattering can be obtained at the same time. In the current work, The invariant mass spectrum of $\Lambda J/\psi$ channel can be given approximately with the scattering amplitude $\mathcal{M}_{J/\psi\Lambda}^{J^P}$ as [60,61],

$$\frac{d\Gamma}{dW} = \sum_{J^P} C_{J^P} \sum_{\lambda' \geq 0, \lambda \geq 0} |\mathcal{M}_{J/\psi\Lambda, \lambda'\lambda}^{J^P}(\mathbf{p}', \mathbf{p})|^2 \cdot \lambda^{\frac{1}{2}}(W, m_{J/\psi}, m_\Lambda) \lambda'^{\frac{1}{2}}(\tilde{W}, W, m_3)/W, \quad (14)$$

with \tilde{W} being total energy of the decay process, that is, the mass of Ξ_b^- baryon or B^- meson. For simplicity, we do not calculate the yield of initial decay process from Ξ_b^- baryon or B^- meson, and a yield parameter C_{J^P} for spin parity J^P is introduced to absorb all uncertainties and the information about the yield.

III. RESULT AND DISCUSSION

A. Bound states from single-channel calculation

The hadronic molecular state is a bound state from the interaction of two hadrons. The single-channel calculation will provide the basic picture of molecular states from the interaction considered. Here, a search for the poles from single-channel interactions will be first performed by the $\log|1 - V(z)G(z)|$ with the variation of real and imaginary parts of z . The results with a cutoff $\Lambda = 1.1$ GeV are presented in Fig. 1, where the abscissa corresponds to the real part of the pole position, and the ordinate corresponds to the imaginary part of the pole position. In this work, we only consider the bound states which can be introduced in S wave. However, in the calculation, higher-wave contributions for these states are included.

There are five poles found from the interactions considered in energy region from 4200 to 4550 MeV. Since only single-channel interactions are considered, all poles are found on the real axis of the complex energy plane. These poles correspond to the five molecular states generated from the single-channel interaction of $\Xi_c^* \bar{D}$ with spin parity $J^P = 3/2^-, \Xi_c \bar{D}^*$ with $1/2^-$ and $3/2^-$, $\Xi_c' \bar{D}$ with $1/2^-$, and $\Xi_c \bar{D}$ with $1/2^-$. If the cutoff increases, all poles will leave corresponding thresholds further. Two states with $1/2^-$ and $3/2^-$ from the $\Xi_c \bar{D}^*$ interaction have almost the same mass with single-channel calculation, about 4474 MeV, which is a little larger than that of $P_{\psi_s}^\Lambda(4459)$. They only can be distinguished after considering coupling effects and the cutoff Λ also should be adjusted a little larger. The $\Xi_c \bar{D}(1/2^-)$ interaction can produce an S-wave bound state with a mass of about 4335 MeV, which is very close to the mass of $P_{\psi_s}^\Lambda(4338)$. The $\Xi_c' \bar{D}$ interaction produces a

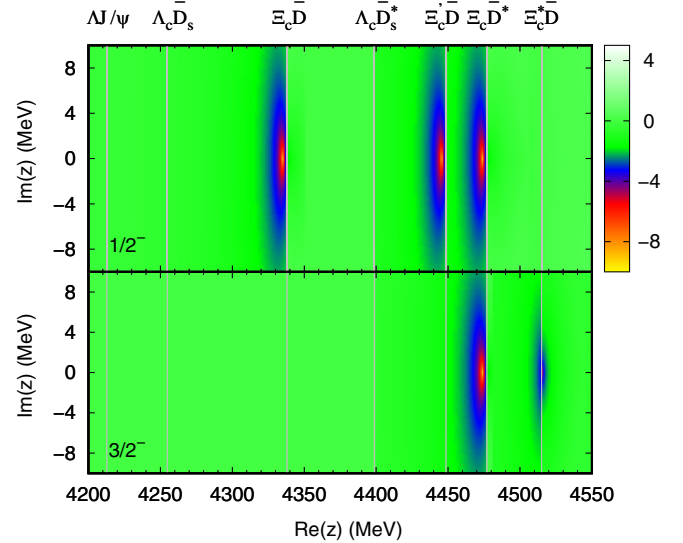


FIG. 1. Poles with spin parities $1/2^-$ (upper panel) and $3/2^-$ (lower panel) from the single-channel interactions. The gray lines correspond to the thresholds of the interactions. The color box is for the $\log|1 - V(z)G(z)|$.

molecular state with spin parity $1/2^-$. The $\Xi_c^* \bar{D}$ channel produces a molecular state with spin parity $3/2^-$, which has relatively weaker attraction than the other four states. Its mass is almost at the threshold, but the binding energy will increase with the increase of cutoff. Since there is no light meson exchange potential as the attractive mechanism, the rest three channels $\Lambda_c \bar{D}_s^*$, $\Lambda_c \bar{D}_s$, and $\Lambda J/\psi$ cannot be bound in the current model even if the cutoff Λ is adjusted to the largest value in reasonable range.

B. States near $\Xi_c \bar{D}^*$ threshold and $P_{\psi_s}^\Lambda(4459)$

For better understanding of the origin of the $P_{\psi_s}^\Lambda(4459)$, the coupled-channel effects will be included to introduce width to the bound states and estimate the $J/\psi\Lambda$ invariant mass spectrum in energy region of [4360 – 4540] MeV where the $P_{\psi_s}^\Lambda(4459)$ was observed. As shown in the single-channel calculation, four molecular states are produced in this energy region, including $\Xi_c' \bar{D}(1/2^-)$, $\Xi_c \bar{D}^*(1/2^-, 3/2^-)$, and $\Xi_c^* \bar{D}(3/2^-)$. The yield parameters $C_{1/2^-}$ and $C_{3/2^-}$ are set completely free. To compare with the experimental invariant mass spectrum, the corresponding cutoff Λ will be adjusted to 1.14 GeV, which is a little larger than the one in single-channel calculation, to move the poles to the experimental peak. The cutoff $\Lambda_{(D, D_s)}$ and $\Lambda_{(D^*, D_s^*)}$ will be set as 2.25 and 2.4 GeV, which do not involve in single-channel calculation. With the increase of the cutoff Λ , the binding of states becomes deeper accordingly. The estimated invariant mass spectrum is presented in Fig. 2 and compared with the experiment [24].

In the upper panel of Fig. 2, the theoretical results with a bin of 6 MeV are presented, and compared with the LHCb experiment with the same bin [24]. Besides an obvious

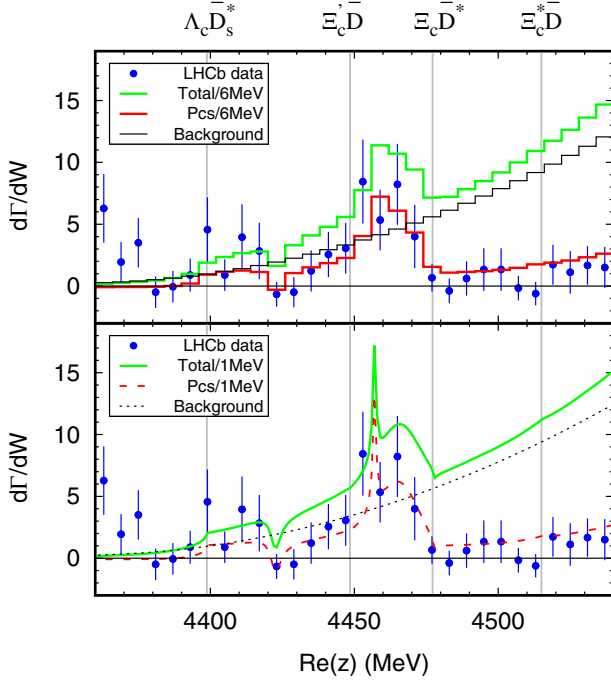


FIG. 2. The $J/\psi\Lambda$ invariant mass spectrums with bin of 6 MeV (upper panel) and of 1 MeV (lower panel). The green, red, and black curves are for the total, peak, and background contributions. The blue points with error bars are the data removing the background contribution from the LHCb experiment [24]. The gray lines correspond to the thresholds of the interactions.

peak from the molecular states, the direct results from the current coupled-channel calculation provide a background contributions in the $J/\psi\Lambda$ invariant mass spectrum (see green curves in Fig. 2). It is simply removed as a unary quadratic function $BK(W) = 6646.84 - 3053.5W + 350.7W^2$ by comparing the theoretical and experimental results in the energy region of $[4360 - 4390] \cup [4480 - 4540]$ MeV (see black curves in Fig. 2). After removing such background, the results from the molecular states are extracted, and in good line with the experimental data. To find the best comparison with experiment with bin of 6 MeV, the contributions of two $\Xi_c\bar{D}^*$ states with spin parity $1/2^-$ and $3/2^-$ exhibit as one peak. If we adjust bin to a smaller value, 1 MeV, in the lower panel of Fig. 2, the contributions from the two states are distinguishable. It shows that the peak of $P_{\psi s}^\Lambda(4459)$ may be composed of a higher narrow $\Xi_c\bar{D}^*$ state with $J^P = 3/2^-$ and a lower wider $\Xi_c\bar{D}^*$ state with $J^P = 1/2^-$.

To provide more explicit of the contributions from these two $\Xi_c\bar{D}^*$ states, the poles and the invariant mass spectrum for different spin parities will be presented. The results for spin parity $1/2^-$ is illustrated in Fig. 3. In the single-channel calculation, where two poles are found on the real axis near the $\Xi_c'\bar{D}$ and $\Xi_c\bar{D}^*$ thresholds, respectively. After including the coupled-channel effect, the poles leave the real axis and become two conjugate poles in the complex energy planes,

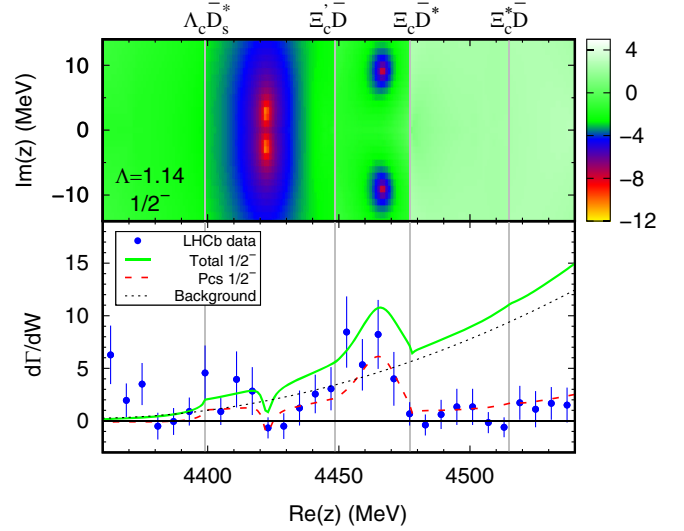


FIG. 3. The poles (upper panel) and the $J/\psi\Lambda$ invariant mass spectrum (lower panel) for spin parity $1/2^-$. The green (full), red (dashed), and black (dotted) curves are for the total, peak, and background contributions. The blue points with error bars are the data removing the background contribution from the LHCb experiment cited from Ref. [24]. The gray lines correspond to the thresholds of the interactions.

which indicates that the bound states acquire width. The $\Xi_c\bar{D}^*$ state with spin parity $1/2^-$ has a mass of 4465 MeV and a width of 18 MeV. The structure $P_{\psi s}^\Lambda(4459)$ peak can even be well describe by the peak of state $\Xi_c\bar{D}^*(1/2^-)$, except for the data points at about 4453 MeV. The $\Xi_c'\bar{D}(1/2^-)$ is a relative narrow state at about 4423 MeV with a width of about 6 MeV. In the experimental spectrum, there is a small dip around 4423 MeV, which can be in good conformity with the molecular state $\Xi_c'\bar{D}(1/2^-)$. Unfortunately, the precisions of the experiment are not high enough to identify its existence. The calculation also suggests to observe such state in the $\Lambda_c\bar{D}_s$ invariant mass spectrum.

In Fig. 4, the results for spin parity $3/2^-$ are presented. The $\Xi_c\bar{D}^*$ state with $3/2^-$, as well as that with $1/2^-$, is produced near the threshold with a mass of 4457 MeV. The width of the state $\Xi_c\bar{D}^*(3/2^-)$ equals to about 1.6 MeV, being much smaller than that of the state with $1/2^-$. The peak of the state $\Xi_c\bar{D}^*(3/2^-)$ is so narrow that it can only raise the events near the central value and not affect much of the general shape of the invariant mass spectrum. The peak with cutoff $\Lambda = 1.14$ falls in the middle of two highest data points. If a little larger cutoff $\Lambda = 1.18$ is adopted, the peak will move to the lower highest data point. The state $\Xi_c^*\bar{D}(3/2^-)$ has a mass of about 4512 MeV and a width of about 17 MeV. The low yield of the events with $J^P = 3/2^-$ indicates that high precision data are required to observe the $\Xi_c^*\bar{D}(3/2^-)$ in $J/\psi\Lambda$ invariant mass spectrum. The decay channels $\Xi_c\bar{D}^*$ and $\Lambda_c\bar{D}_s^*$ couple strongly with the state, which will be good choices to search for this state.

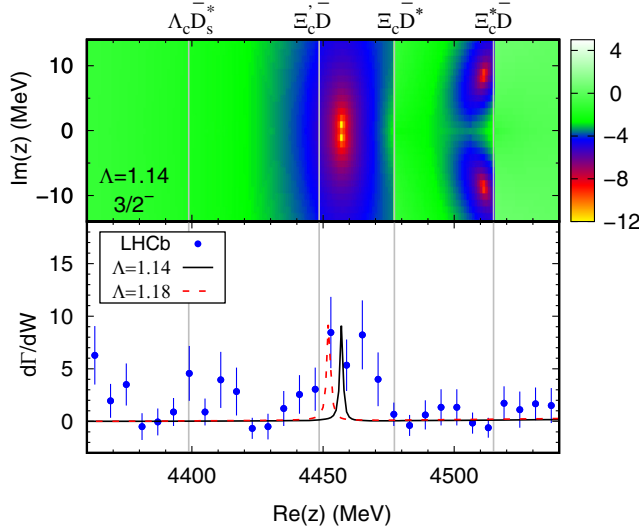


FIG. 4. The poles (upper panel) and $J/\psi\Lambda$ invariant mass spectrum (lower panel) for spin parity $1/2^-$. The black (full) and red (dashed) lines are for the peak from the coupled-channel interactions with cutoff 1.14 and 1.18, respectively. The blue points with error bars are the data removing the background contribution from LHCb experiment [24]. The gray lines correspond to the thresholds of the interactions.

C. State near $\Xi_c\bar{D}$ threshold and $P_{\psi s}^\Lambda(4338)$

The $P_{\psi s}^\Lambda(4338)$ was observed near the $\Xi_c\bar{D}$ threshold in the process $B^- \rightarrow J/\psi\Lambda\bar{p}$. The single-channel results suggest a bound state from the $\Xi_c\bar{D}$ interaction, which is close to the $P_{\psi s}^\Lambda(4338)$. To confirm their relation, the invariant mass spectrum is estimated and compared with the experiment. To match the experimental data points, we need to introduce a parametrized background contribution of a form $M_{\Lambda J/\psi}^{BK, J^P} = a e^{ib\pi} (M_{\Lambda J/\psi} - M_{\min})^c (M_{\max} - M_{\Lambda J/\psi})^d$ with the M_{\max} and M_{\min} being the upper and lower limits of phase space, which interferes with the amplitude from the $\Xi_c\bar{D}$ interaction. Considering that the $P_{\psi s}^\Lambda(4338)$ is very close to the threshold, the cutoff Λ is adjusted to 1.04 GeV, a little smaller than 1.1 GeV, and the cutoff $\Lambda_{(D, D_s)}$ and $\Lambda_{(D^*, D_s^*)}$ will be set as 2.15 and 2.3 GeV. The parameters for the background will be set as $(a, b, c, d) = (0.054, 0.19, 0.085, 0.28)$. The yield parameter $C_{1/2^-}$ is set completely free. The results are shown in the following Fig. 5 and compared with recent LHCb experiment.

The diagram of poles shows that a very narrow molecular state from the $\Xi_c\bar{D}$ interaction with spin parity $1/2^-$, which is very close to the corresponding threshold. The mass and width of the state are about 4336.5 MeV and 0.8 MeV, respectively. The strong coupling between the $\Lambda_c\bar{D}_s$ and the $\Xi_c\bar{D}$ channels provides the dominant contribution of its width. In the $J/\psi\Lambda$ invariant mass spectrum, the angle of interference between them has reached about 34.2° .

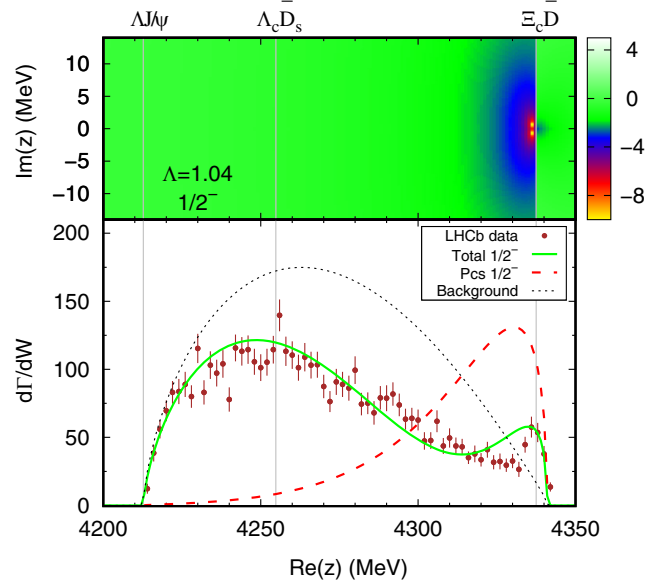


FIG. 5. The poles (upper panel) and $J/\psi\Lambda$ invariant mass spectrum (lower panel) for spin parity $1/2^-$. The green (full), red (dashed), and black (dotted) curves are for the total, peak, and background contributions. The brown points with error bars are the data removing the background contribution from the LHCb experiment [29]. The gray lines correspond to the thresholds of the interactions.

Since the pole is very close to the real axis, a very narrow peak can be produced from the square of the amplitudes $|\mathcal{M}_{J/\psi\Lambda, \lambda\lambda'}^{J^P}(p', p)|^2$ in Eq. (14). However, the pole produced from the $\Xi_c\bar{D}$ interaction is close to the threshold of the phase space. The original narrow peak is suppressed into a relatively wide peak by the factor $\lambda'(\bar{W}, W, m_3)$. Such a result implies that the width of $P_{\psi s}^\Lambda(4338)$ determined experimentally need more analysis. An obvious enhancement can be produced from the contribution of molecular state $\Xi_c\bar{D}(1/2^-)$. Obviously, the structure $P_{\psi s}^\Lambda(4338)$ is in line with the molecular state of $\Xi_c\bar{D}(1/2^-)$. The peak from the molecular state seems obvious wider than the experimental structure. In Ref. [35], more contributions, such as threshold cusp effects, are included. The line shape in the no-pole model suggests the $\Xi_c\bar{D}$ threshold cusp plays important role in the $P_{\psi s}^\Lambda(4338)$ peak structure. The inclusion of those contributions may be helpful to better understand the sharp peak structure. It seems that more elaborate structures like $\Xi_c^+ D^-$ and $\Xi_c^0 \bar{D}^0$ channels under the uncoupled isospin representation is also helpful to obtain a sharp peak as discussed in Ref. [39]. Besides, if the strong coupling between $\Lambda_c\bar{D}_s$ and $\Xi_c\bar{D}$ channels is weakened, the broad bump can also become a narrow peak. However, in the current work, there is only one adjustable parameter Λ , it is impossible to weaken the coupling of certain two channels but keep strengths of other interactions unchanged.

IV. SUMMARY

In this work, we perform a coupled-channel calculation to study the molecular states produced from interactions $\Xi_c^* \bar{D}^*$, $\Xi_c' \bar{D}^*$, $\Xi_c^* \bar{D}$, $\Xi_c' \bar{D}$, $\Lambda_c \bar{D}_s^*$, $\Xi_c \bar{D}$, $\Lambda_c \bar{D}_s$, and $\Lambda J/\psi$. The poles of the molecular states are searched in complex energy plane in the qBSE approach. With the help of effective Lagrangian, the potential kernel can be constructed by meson exchanges. With the scattering amplitudes obtained, the invariant mass spectra are estimated and compared with the experiment. Based on the current results, the understanding of the experimentally observed $P_{\psi s}^\Lambda(4459)$ and $P_{\psi s}^\Lambda(4438)$, as well as their partners, can be drawn as follows.

- (i) The $\Xi_c \bar{D}^*$ state with spin parity $1/2^-$ can reproduce the general line shape of the structure $P_{\psi s}^\Lambda(4459)$ in the $J/\psi\Lambda$ invariant mass spectrum. However, the contribution from the $\Xi_c \bar{D}^*$ state with $3/2^-$, which is lower than the $1/2^-$ state, cannot be excluded due to its very small width. The high-precision data is required to understand its role in this structure.
- (ii) Based on the $J/\psi\Lambda$ invariant mass spectrum, the existence of $P_{\psi s}^\Lambda(4459)$ suggests a dip near the $\Xi_c' \bar{D}$ threshold in the LHCb experimental data. Such dip is consistent with a $\Xi_c' \bar{D}$ molecular state with $1/2^-$ with a mass of 4423 MeV and a width of 6 MeV. The $\Lambda_c D_s$ channel is a good place to search for this state.
- (iii) The state $\Xi_c^* \bar{D}(3/2^-)$ can be produced from the coupled channel calculation with a mass of 4512 MeV and a width of 17 MeV. However, both experimental and theoretical results suggest that it couples very weakly to the $\Lambda J/\psi$ channel. It is

suggested to search for such state in the channels $\Xi_c \bar{D}^*$ and $\Lambda_c D_s^*$.

- (iv) A molecular state with a very small width can be produced from the $\Xi_c \bar{D}$ interaction with spin parity $(1/2^-)$, which is very close to the $P_{\psi s}^\Lambda(4338)$. Obviously, the structure $P_{\psi s}^\Lambda(4338)$ is in line with the molecular state of $\Xi_c \bar{D}(1/2^-)$. The phase space suppress it into a wider peak near the threshold. Large interference with background should be introduced to reproduce a narrow peak. The $\Xi_c \bar{D}$ threshold cusp effect may be also important to cause the peak [35]. In addition, the molecular state $\Xi_c \bar{D}(1/2^-)$ also can be search for in the $\Lambda_c D_s$ channel.
- (v) Within the current model, there is no bound state produced from the interactions $\Lambda_c \bar{D}_s^*$, $\Lambda_c \bar{D}_s$, and $\Lambda J/\psi$.

The current calculation is performed with only the contribution of molecular states from coupled-channel interactions and a parametrized background. Other contributions, such as the cusp effects, are not included. The initial decay processes are also parametrized as free parameters. To better understand the roles of the molecular states in such decays and their relations to the observed structures, inclusion of more contributions will be helpful.

ACKNOWLEDGMENTS

This project is supported by the Postgraduate Research and Practice Innovation Program of Jiangsu Province (Grants No. KYCX21_1323) and the National Natural Science Foundation of China (Grants No. 11675228).

-
- [1] R. Aaij *et al.* (LHCb Collaboration), Observation of $J/\psi p$ Resonances Consistent with Pentaquark States in $\Lambda_b^0 \rightarrow J/\psi K^- p$ Decays, *Phys. Rev. Lett.* **115**, 072001 (2015).
 - [2] J. J. Wu, R. Molina, E. Oset, and B. S. Zou, Prediction of Narrow N^* and Λ^* Resonances with Hidden Charm Above 4 GeV, *Phys. Rev. Lett.* **105**, 232001 (2010).
 - [3] Z. C. Yang, Z. F. Sun, J. He, X. Liu, and S. L. Zhu, The possible hidden-charm molecular baryons composed of anti-charmed meson and charmed baryon, *Chin. Phys. C* **36**, 6 (2012).
 - [4] W. L. Wang, F. Huang, Z. Y. Zhang, and B. S. Zou, $\Sigma_c \bar{D}$ and $\Lambda_c \bar{D}$ states in a chiral quark model, *Phys. Rev. C* **84**, 015203 (2011).
 - [5] C. W. Xiao, J. Nieves, and E. Oset, Combining heavy quark spin and local hidden gauge symmetries in the dynamical generation of hidden charm baryons, *Phys. Rev. D* **88**, 056012 (2013).
 - [6] H. X. Chen, W. Chen, X. Liu, and S. L. Zhu, The hidden-charm pentaquark and tetraquark states, *Phys. Rep.* **639**, 1 (2016).
 - [7] F. K. Guo, C. Hanhart, U. G. Meißner, Q. Wang, Q. Zhao, and B. S. Zou, Hadronic molecules, *Rev. Mod. Phys.* **90**, 015004 (2018).
 - [8] R. Aaij *et al.* (LHCb Collaboration), Observation of a Narrow Pentaquark State, $P_c(4312)^+$, and of Two-Peak Structure of the $P_c(4450)^+$, *Phys. Rev. Lett.* **122**, 222001 (2019).
 - [9] R. Chen, X. Liu, X. Q. Li, and S. L. Zhu, Identifying Exotic Hidden-Charm Pentaquarks, *Phys. Rev. Lett.* **115**, 132002 (2015).
 - [10] H. X. Chen, W. Chen, X. Liu, T. G. Steele, and S. L. Zhu, Towards Exotic Hidden-Charm Pentaquarks in QCD, *Phys. Rev. Lett.* **115**, 172001 (2015).
 - [11] M. Karliner and J. L. Rosner, New Exotic Meson and Baryon Resonances from Doubly-Heavy Hadronic Molecules, *Phys. Rev. Lett.* **115**, 122001 (2015).

- [12] L. Roca, J. Nieves, and E. Oset, LHCb pentaquark as a $\bar{D}^*\Sigma_c - \bar{D}^*\Sigma_c^*$ molecular state, *Phys. Rev. D* **92**, 094003 (2015).
- [13] J. He, $\bar{D}^*\Sigma_c^*$ and $\bar{D}^*\Sigma_c$ interactions and the LHCb hidden-charmed pentaquarks, *Phys. Lett. B* **753**, 547 (2016).
- [14] T. J. Burns, Phenomenology of $P_c(4380)^+$, $P_c(4450)^+$ and related states, *Eur. Phys. J. A* **51**, 152 (2015).
- [15] V. V. Anisovich, M. A. Matveev, J. Nyiri, A. V. Sarantsev, and A. N. Semenova, Nonstrange and strange pentaquarks with hidden charm, *Int. J. Mod. Phys. A* **30**, 1550190 (2015).
- [16] Z. G. Wang, Analysis of the $\frac{1}{2}^\pm$ pentaquark states in the diquark–diquark–antiquark model with QCD sum rules, *Eur. Phys. J. C* **76**, 142 (2016).
- [17] A. Feijoo, V. K. Magas, A. Ramos, and E. Oset, A hidden-charm $S = -1$ pentaquark from the decay of Λ_b into $J/\psi, \eta\Lambda$ states, *Eur. Phys. J. C* **76**, 446 (2016).
- [18] J. X. Lu, E. Wang, J. J. Xie, L. S. Geng, and E. Oset, The $\Lambda_b \rightarrow J/\psi K^0\Lambda$ reaction and a hidden-charm pentaquark state with strangeness, *Phys. Rev. D* **93**, 094009 (2016).
- [19] H. X. Chen, L. S. Geng, W. H. Liang, E. Oset, E. Wang, and J. J. Xie, Looking for a hidden-charm pentaquark state with strangeness $S = -1$ from Ξ_b^- decay into $J/\psi K^-\Lambda$, *Phys. Rev. C* **93**, 065203 (2016).
- [20] R. Chen, J. He, and X. Liu, Possible strange hidden-charm pentaquarks from $\Sigma_c^{(*)}\bar{D}_s^*$ and $\Xi_c^{(*)}\bar{D}^*$ interactions, *Chin. Phys. C* **41**, 103105 (2017).
- [21] C. W. Xiao, J. Nieves, and E. Oset, Prediction of hidden charm strange molecular baryon states with heavy quark spin symmetry, *Phys. Lett. B* **799**, 135051 (2019).
- [22] Q. Zhang, B. R. He, and J. L. Ping, Pentaquarks with the $qqs\bar{Q}Q$ configuration in the chiral quark model, [arXiv:2006.01042](https://arxiv.org/abs/2006.01042).
- [23] B. Wang, L. Meng, and S. L. Zhu, Spectrum of the strange hidden charm molecular pentaquarks in chiral effective field theory, *Phys. Rev. D* **101**, 034018 (2020).
- [24] R. Aaij *et al.* (LHCb Collaboration), Evidence of a $J/\psi\Lambda$ structure and observation of excited Ξ^- states in the $\Xi_b^- \rightarrow J/\psi\Lambda K^-$ decay, *Sci. Bull.* **66**, 1278 (2021).
- [25] Z. G. Wang and Q. Xin, Analysis of hidden-charm pentaquark molecular states with and without strangeness via the QCD sum rules *, *Chin. Phys. C* **45**, 123105 (2021).
- [26] H. X. Chen, W. Chen, X. Liu, and X. H. Liu, Establishing the first hidden-charm pentaquark with strangeness, *Eur. Phys. J. C* **81**, 409 (2021).
- [27] R. Chen, Can the newly reported $P_{cs}(4459)$ be a strange hidden-charm $\Xi_c\bar{D}^*$ molecular pentaquark?, *Phys. Rev. D* **103**, 054007 (2021).
- [28] F. Z. Peng, M. J. Yan, M. Sánchez Sánchez, and M. P. Valderrama, The $P_{cs}(4459)$ pentaquark from a combined effective field theory and phenomenological perspective, *Eur. Phys. J. C* **81**, 666 (2021).
- [29] LHCb Collaboration, Observation of a $J/\psi\Lambda$ resonance consistent with a strange pentaquark candidate in $B^- \rightarrow J/\psi\Lambda\bar{p}$ decays, [arXiv:2210.10346](https://arxiv.org/abs/2210.10346).
- [30] X. W. Wang and Z. G. Wang, Analysis of the $P_{cs}(4338)$ and related pentaquark molecular states via the QCD sum rules, *Chin. Phys. C* **47**, 013109 (2023).
- [31] F. L. Wang and X. Liu, Emergence of molecular-type characteristic spectrum of hidden-charm pentaquark with strangeness embodied in the $P_{\psi_s}^\Lambda(4338)$ and $P_{cs}(4459)$, *Phys. Lett. B* **835**, 137583 (2022).
- [32] M. J. Yan, F. Z. Peng, M. Sánchez Sánchez, and M. Pavon Valderrama, The $P_{\psi_s}^\Lambda(4338)$ pentaquark and its partners in the molecular picture, [arXiv:2207.11144](https://arxiv.org/abs/2207.11144).
- [33] U. Özdem, Investigation of magnetic moment of $P_{cs}(4338)$ and $P_{cs}(4459)$ molecular pentaquarks, *Phys. Lett. B* **836**, 137635 (2023).
- [34] F. L. Wang, H. Y. Zhou, Z. W. Liu, and X. Liu, What can we learn from the electromagnetic properties of hidden-charm molecular pentaquarks with single strangeness?, *Phys. Rev. D* **106**, 054020 (2022).
- [35] S. X. Nakamura and J. J. Wu, Pole determination of $P_{\psi_s}^\Lambda(4338)$ and possible $P_{\psi_s}^\Lambda(4254)$ in $B^- \rightarrow J/\psi\Lambda\bar{p}$, [arXiv:2208.11995](https://arxiv.org/abs/2208.11995).
- [36] A. Giachino, A. Hosaka, E. Santopinto, S. Takeuchi, M. Takizawa, and Y. Yamaguchi, Rich structure of the hidden-charm pentaquarks near threshold regions, [arXiv:2209.10413](https://arxiv.org/abs/2209.10413).
- [37] P. G. Ortega, D. R. Entem, and F. Fernandez, Strange hidden-charm $P_{\psi_s}^\Lambda(4459)$ and $P_{\psi_s}^\Lambda(4338)$ pentaquarks and additional $P_{\psi_s}^\Lambda$, $P_{\psi_s}^\Sigma$ and $P_{\psi_s}^N$ candidates in a quark model approach, *Phys. Lett. B* **838**, 137747 (2023).
- [38] T. J. Burns and E. S. Swanson, The LHCb state $P_{\psi_s}^\Lambda(4338)$ as a triangle singularity, *Phys. Lett. B* **838**, 137715 (2023).
- [39] L. Meng, B. Wang, and S. L. Zhu, The double thresholds distort the lineshapes of the $P_{\psi_s}^\Lambda(4338)^0$ resonance, *Phys. Rev. D* **107**, 014005 (2023).
- [40] J. T. Zhu, L. Q. Song, and J. He, $P_{cs}(4459)$ and other possible molecular states from $\Xi_c^{(*)}\bar{D}^{(*)}$ and $\Xi_c'\bar{D}^{(*)}$ interactions, *Phys. Rev. D* **103**, 074007 (2021).
- [41] H. Y. Cheng, C. Y. Cheung, G. L. Lin, Y. C. Lin, T. M. Yan, and H. L. Yu, Chiral Lagrangians for radiative decays of heavy hadrons, *Phys. Rev. D* **47**, 1030 (1993).
- [42] T. M. Yan, H. Y. Cheng, C. Y. Cheung, G. L. Lin, Y. C. Lin, and H. L. Yu, Heavy quark symmetry and chiral dynamics, *Phys. Rev. D* **46**, 1148 (1992); **55**, 5851(E) (1997).
- [43] M. B. Wise, Chiral perturbation theory for hadrons containing a heavy quark, *Phys. Rev. D* **45**, R2188 (1992).
- [44] R. Casalbuoni, A. Deandrea, N. Di Bartolomeo, R. Gatto, F. Feruglio, and G. Nardulli, Phenomenology of heavy meson chiral Lagrangians, *Phys. Rep.* **281**, 145 (1997).
- [45] M. Tanabashi *et al.* (Particle Data Group), Review of particle physics, *Phys. Rev. D* **98**, 030001 (2018).
- [46] R. Chen, Z. F. Sun, X. Liu, and S. L. Zhu, Strong LHCb evidence supporting the existence of the hidden-charm molecular pentaquarks, *Phys. Rev. D* **100**, 011502 (2019).
- [47] Y. R. Liu and M. Oka, $\Lambda_c N$ bound states revisited, *Phys. Rev. D* **85**, 014015 (2012).
- [48] C. Isola, M. Ladisa, G. Nardulli, and P. Santorelli, Charming penguins in $B \rightarrow K^*\pi, K(\rho, \omega, \phi)$ decays, *Phys. Rev. D* **68**, 114001 (2003).
- [49] A. F. Falk and M. E. Luke, Strong decays of excited heavy mesons in chiral perturbation theory, *Phys. Lett. B* **292**, 119 (1992).
- [50] A. Mueller-Groeling, K. Holinde, and J. Speth, K- N interaction in the meson exchange framework, *Nucl. Phys.* **A513**, 557 (1990).

- [51] R. Molina, D. Nicmorus, and E. Oset, The rho rho interaction in the hidden gauge formalism and the $f_0(1370)$ and $f_2(1270)$ resonances, *Phys. Rev. D* **78**, 114018 (2008).
- [52] C. W. Shen, D. Rönchen, U. G. Meißner, and B. S. Zou, Exploratory study of possible resonances in heavy meson—Heavy baryon coupled-channel interactions, *Chin. Phys. C* **42**, 023106 (2018).
- [53] C. W. Shen, J. J. Wu, and B. S. Zou, Decay behaviors of possible $\Lambda_{c\bar{c}}$ states in hadronic molecule pictures, *Phys. Rev. D* **100**, 056006 (2019).
- [54] J. He and D. Y. Chen, Molecular states from $\Sigma_c^{(*)}\bar{D}^{(*)} - \Lambda_c\bar{D}^{(*)}$ interaction, *Eur. Phys. J. C* **79**, 887 (2019).
- [55] F. Gross and A. Stadler, Covariant spectator theory of np scattering: Phase shifts obtained from precision fits to data below 350 MeV, *Phys. Rev. C* **78**, 014005 (2008).
- [56] J. He, The $Z_c(3900)$ as a resonance from the $D\bar{D}^*$ interaction, *Phys. Rev. D* **92**, 034004 (2015).
- [57] J. He, Study of the $B\bar{B}^*/D\bar{D}^*$ bound states in a Bethe-Salpeter approach, *Phys. Rev. D* **90**, 076008 (2014).
- [58] J. He, D. Y. Chen, and X. Liu, New structure around 3250 MeV in the Baryonic B decay and the $D_0^*(2400)N$ molecular hadron, *Eur. Phys. J. C* **72**, 2121 (2012).
- [59] L. Roca, E. Oset, and J. Singh, Low lying axial-vector mesons as dynamically generated resonances, *Phys. Rev. D* **72**, 014002 (2005).
- [60] F. Aceti, M. Bayar, E. Oset, A. Martinez Torres, K. P. Khemchandani, J. M. Dias, F. S. Navarra, and M. Nielsen, Prediction of an $I = 1$ $D\bar{D}^*$ state and relationship to the claimed $Z_c(3900)$, $Z_c(3885)$, *Phys. Rev. D* **90**, 016003 (2014).
- [61] T. Hyodo, A. Hosaka, E. Oset, A. Ramos, and M. J. Vicente Vacas, $\Lambda(1405)$ production in the $\pi^- p \rightarrow K^0 \pi \Sigma$ reaction, *Phys. Rev. C* **68**, 065203 (2003).